Quantifying the Variable Effects of Systems with Demand Response Resources

Anupama Kowli and George Gross
Department of Electrical and Computer Engineering
University of Illinois, Urbana, Illinois 61801, USA

***Abstract*—The growing environmental concerns and increasing electricity prices have led to wider implementation of demand-side activities and created a new class of consumers, called demand response resources (*DRR*s). The *DRR*s actively participate in the electricity markets as buyers of electricity and sellers of load curtailment services. The demand profile modifications resulting from the *DRR* curtailments affect the market outcomes and impact the generation and transmission resource utilization. In this paper, we propose a computationally efficient simulation approach to quantify the impacts of *DRR*s on market performance, generation dispatch, transmission usage, environment and other system variable effects. We focus on the variable effects that are of interest in planning and policy analysis studies. We construct the proposed simulation approach by marrying the concepts of probabilistic simulation with snapshot-based analysis techniques. In this way, we effectively integrate the representation of the supply- and demand-side resources, electricity markets, transmission grid operations and constraints, and various sources of uncertainty in the simulation. We discuss the implementation aspects of the proposed approach to ensure computational tractability so as to allow its application to the simulation of large-scale systems over longer-term periods. We discuss representative simulation results to illustrate the application of the proposed approach to quantification of the variable effects of a large-scale test system. The reported results demonstrate the economic, environmental and reliability benefits the integration of *DRR*s can provide to the test system.**

I. Introduction

The push towards sustainability, increasing electricity prices, technological advances and policy initiatives at the federal and state level drive the efforts to harness active participation of the consumers in the North American electricity markets [1]. Such efforts have lead towards the implementation several demand-side activities which, in turn, have created many new players in the electricity industry. In particular, there is a new class of consumers, called *demand response resources* (*DRR*s), whose role has become increasingly important in ensuring that the supply-demand balance is efficiently attained [2], [3]. In addition to purchasing electricity from the markets, the *DRR*s can sell load curtailment services to the markets by reducing their loads during certain hours. For these hours, the *DRR*s compete to provide the load curtailment services directly against the supply-side resources that sell their generation outputs and provide the *IGO* with additional degrees of freedom in maintaining economic and reliable operation of the power system. The *time-dependent DRR* deployments impact the loading on the system, thereby impacting the generation and transmission resource utilization as well as the market outcomes.

The potential load reduction from the *DRR*s in the year 2008 was estimated to be close to 41 *GW*, which represented approximately 5.8 % of 2008 U.S. peak load [4]. This capacity is significant in terms of preventing the need for the use of some existing and the possible construction of new peaking units as well as deferring the need for new transmission capacity [5], [6]. The implementation of the smart grid with a deeper penetration of renewable supply resources is expected to entail a broader deployment of *DRR*s [7]. Indeed, the projections of the peak load reductions potential in 2019 range between 38 GW and 188 GW across the country, which roughly constitutes about 4 to 20 % of the nation-wide peak demand [8]. As the penetration of *DRR*s deepens, their impacts on market outcomes and system operations become more pronounced and propagate to generation and transmission planning and, eventually, entail regulatory/legislative initiatives. Consequently, there is a need for appropriate tools for quantifying the impacts of *DRR*s on market performance, generation dispatch, transmission usage, emissions and other system variable effects. A particularly critical requirement is that of a simulation tool to emulate the behavior of a power system with integrated *DRR*s; we address this requirement. We present, in this paper, the development of a simulation approach that provides the basis of such a tool. We illustrate the application of the proposed approach to various planning and analysis studies.

While the impacts of *DRR*s on the system variable effects over short- and medium-term periods have been studied to some extent [9]–[15], our focus is on the longer-term study periods. We are interested in assessing the impacts of *DRR*s on the variable effects that are typically evaluated in planning and policy analysis studies. Consequently, explicit representation of the various sources of uncertainty which impact system and market operations along with the representation, with the appropriate level of detail, of the supply- and demand-side resources, the transmission grid, the market clearing operations, the market structure and operating policies, is the key requirement of the simulation approach.

We develop a systematic, computationally efficient approach that allows the representation of the time-dependent nature of the *DRR* deployments and the transmission-constrained market clearing operations as well as that of the uncertainty inherent in power systems and the policies in effect. Our approach is designed to be applicable to longer-term analysis and to capture the uncertainty in future developments. The time-dependent nature of *DRR*s leads to the use of the snapshot-based market performance analysis as the basic building block of the proposed approach. Given the longer-term nature of the studies, we make use of probabilistic simulation concepts and the associated uniformity assumptions in the construction of the approach. In this way, we capture the effects of uncertainty on the system and market operations. In the implementation of the proposed approach, we pay careful attention to reducing the computationally demanding work. For this purpose, we devise effective means to specify the simulation periods and also use *Latin hypercube sampling* scheme to provide an efficient way to approximate the probability distributions of the market outcomes. Thus, we bring about computational tractability in the quantification of the system variable effects; particularly those of large-scale systems over longer-term periods.

The proposed approach provides, for the first time, a useful mechanism to assess the impacts of effective *DRR* utilization on resource investment decisions, transmission planning and system reliability. The approach has a wide range of applications – from justifying investments in *DRR*s to investigating dynamic pricing schemes, from formulating policies for the more widespread use of demand-side resources to devising effective strategies for their utilization and from study of alternative market designs to quantifying environmental benefits of the smart grid implementations. The proposed approach is useful for *IGO*s, *ESP*s, generation and transmission asset investors, regulators and policy makers to make better informed decisions.

The paper contains five additional sections. We describe in section II the modeling details and in section III the proposed approach. In section IV, we discuss the implementation steps to bring about computational tractability in the practical applications of our approach. We report representative application studies in section V in which we demonstrate the capability of the proposed approach to quantitatively assess the range of *DRR* impacts on a large test system. We conclude with a summary and directions for future work in section VI.

II. Models and Metrics

We devote this section to the description of the models and metrics used in our approach. At the outset, we state the assumptions we impose on all the relevant aspects of the problem for modeling purposes. We assume that throughout the simulation period the resource mix, the transmission grid, the market structure, the operating policies and the seasonality effects remain unchanged so that the loads and the resources exhibit uniform characteristics. We assume that a forecast of the aggregate system load consisting both fixed and price-sensitive load components is specified for the simulation period and that each component is known. To simplify the discussion, we consider the supply system to consist of only controllable, i.e., dispatchable units. We assume that the impacts of the unit commitment decisions over the simulation period are incorporated into the specified loading list of the supply resources (*SR*s). We also assume that the maximum load curtailment capacities offered by the *DRR*s and their associated load recovery impacts are *a priori* specified for a typical weekday (weekend day) and that such diurnal weekday (weekend) *DRR* behavior is assumed valid for each weekday (weekend) of the simulation period. Also, we assume that there is no uncertainty in the availability of the *DRR*s.

We consider the central pool market structure [16] that is widely adopted in many jurisdictions. For the purposes of this study, we assume the behavior of each market participant is unaffected by that of the other participants and we ignore any strategic behavior on the part of either the buyers or the sellers. For market clearing purposes, we consider a lossless transmission network and assume that the *DC* power flow conditions at all times [17]. In the event of insufficient supply due to inadequate resources or forced outages of generators and/or transmission congestion, the *IGO* uses a regulatory specified price cap λ^{max} to clear the market [16]. Whenever such an event occurs, the electricity is priced at λ^{max}.

We consider the day-ahead electricity markets (*DAM*s) and explicitly represent their impacts. We find it convenient, therefore, to adopt an hour as the smallest indecomposable unit of time and we view the system to be in steady-state in each hour in the simulation period. The resolution chosen does not allow the representation of any phenomenon of duration shorter than an hour and, consequently, such phenomena are entirely ignored in the simulation. We denote by $\mathcal{H}$ the index set of the hours $\{1, 2, \ldots, H\}$ in the simulation period, where H is the number of hours. We denote by $\mathcal{H}^c \subset \mathcal{H}$ the subset of hours in which *DRR*s are allowed to submit load curtailment offers. And, we denote by $\mathcal{H}^r \subset \mathcal{H}$, the subset of hours in which *DRR*s are allowed to recover the load curtailments in the hours $h \in \mathcal{H}^c$. We impose the restriction $\mathcal{H}^r \cap \mathcal{H}^c = \emptyset$ so that the beneficial effects of load curtailments are not attenuated due to load recovery actions [9], [10].

We review the *IGO*'s market clearing problem for a specified hour $h \in \mathcal{H}$ such that $h \notin \mathcal{H}^c$ and $h \notin \mathcal{H}^r$. We use $\mathcal{S}$ ($\mathcal{B}$) to denote the collection of supply-side sellers (demand-side buyers). Each seller (buyer) submits its price and quantity offer (bid), indicating the willingness to sell to (buy from) the *IGO* for the hour h. The *IGO* uses this information to clear the hour h market. The market clearing depends on the physical network [18] and, therefore, we require a representation of the transmission grid for the assessment of market performance.

We consider the transmission grid to consist of $(N+1)$ buses with J transmission lines. We use the set $\mathcal{N} = \{0, 1, \ldots, N\}$ to denote the index set of the buses in the network, with bus 0 denoting the slack bus. We denote by $\mathscr{J} = \{1, 2, \ldots, J\}$ the index set of the lines and the transformers which connect the buses of the network. We associate with each line/transformer $j \in \mathscr{J}$ the real power flow limit f_j^{max}. We denote by $\underline{\boldsymbol{A}}$ the $J \times N$ reduced branch-to-node incidence matrix, by $\underline{\boldsymbol{B}}_d$ the $J \times J$ diagonal branch susceptance matrix, by $\underline{\boldsymbol{B}}$ the $N \times N$ reduced nodal susceptance matrix and by $\underline{\boldsymbol{b}}_0$ the $N \times 1$ column vector of the augmented susceptance matrix corresponding to the slack node. We use $\underline{\boldsymbol{A}}$, $\underline{\boldsymbol{B}}_d$, $\underline{\boldsymbol{B}}$ and $\underline{\boldsymbol{b}}_0$ in the expressions for the *DC* power flow equations and transmission constraints [18] to describe the key characteristics of the transmission system for the hour h snapshot.

The market clearing explicitly considers the feasibility of the transactions cleared in the market with respect to the transmission constraints and, determines at each node $n \in \mathcal{N}$, the real power supply (demand) p^g_n (p^d_n). We define the vectors $\underline{\boldsymbol{p}}^g \triangleq [\, p^g_1, p^g_2, \ldots, p^g_N \,]^T$ and $\underline{\boldsymbol{p}}^d \triangleq \left[\, p^d_1, p^d_2, \ldots, p^d_N \,\right]^T$. The *IGO* market clearing for hour h entails the solution of an *OPF* with the objective to maximize the auction surplus[1] $\mathscr{S}$. We use $\beta^b_n(\cdot)$ to represent the aggregated benefits of the buyers at node n and $\gamma^s_n(\cdot)$ to represent the aggregated costs incurred by the *IGO* for the successful offers of the *SR*s at node n. Then, we state the *OPF* as

$$max \ \mathscr{S} = \sum_{n \in \mathcal{N}} \left\{ \beta^b_n(\, p^d_n \,) - \gamma^s_n(\, p^g_n \,) \right\} \tag{1a}$$

$$subject\ to \quad p^g_0 - p^d_0 \ = \underline{\boldsymbol{b}}_0^T \underline{\boldsymbol{\theta}} \quad \leftrightarrow \ \lambda_0 \tag{1b}$$

$$\underline{\boldsymbol{p}}^g - \underline{\boldsymbol{p}}^d \ = \underline{\boldsymbol{B}}\,\underline{\boldsymbol{\theta}} \quad \leftrightarrow \ \underline{\boldsymbol{\lambda}} \tag{1c}$$

$$\underline{\boldsymbol{B}}_d \underline{\boldsymbol{A}}\,\underline{\boldsymbol{\theta}} \ \leq \underline{\boldsymbol{f}}^{max} \quad \leftrightarrow \ \underline{\boldsymbol{\rho}}\,, \tag{1d}$$

with the hour h notation suppressed. We use $\underline{\boldsymbol{\theta}} \triangleq [\, \theta_1, \theta_2, \ldots, \theta_N \,]^T$ and $\underline{\boldsymbol{f}}^{max} \triangleq [\, f^{max}_1, f^{max}_2, \ldots, f^{max}_J \,]^T$ to denote the vectors of the bus voltage phase angles and the real power line flow limits, respectively. We use λ_0, $\underline{\boldsymbol{\lambda}}$ and $\underline{\boldsymbol{\rho}}$ to denote the dual variables associated with the constraints in (1b)-(1d). The constraints and the variables in (1) correspond to the hour h system snapshot.

We denote the *OPF* problem in (1) by $\mathcal{M}(\mathcal{S}, \mathcal{B})\,|_h$. We consider both fixed as well as price-sensitive demand bids in this *OPF* problem which is solved to clear the hour h market. The fixed demand bid, where the buyer exhibits an unlimited willingness to pay for electricity, can be viewed as a special case of the price-sensitive demand bids for which a specified quantity is submitted without price information.

The market performance for the hour h is quantified from the market clearing given by the solution of $\mathcal{M}(\mathcal{S}, \mathcal{B})|_h$. When $\mathcal{M}(\mathcal{S}, \mathcal{B})\,|_h$ is feasible, the optimal values of its decision and dual variables are used to determine the market outcomes. We use $[\, p^g_n \,]^*|_h$ and $[\, p^d_n \,]^*|_h$ to denote the total supply and demand, respectively, cleared at the node n. The total load cleared in hour h is computed as

$$\ell^{\mathcal{S}}|_h \ = \sum_{n \in \mathcal{N}} [\, p^d_n \,]^*|_h \,, \tag{2}$$

which clearly equals the total generation of the supply-side resources. The optimum values $[\, \lambda_n \,]^*|_h$ of the dual variables associated with the nodal power balance constraints provide the locational marginal prices (*LMP*s) at each node $n \in \mathcal{N}$. Each *MWh* is sold (bought) at node n at the price $[\, \lambda_n \,]^*|_h$. Then, the total hourly supply-side payments are

$$w^{\mathcal{S}}|_h \ = \sum_{n \in \mathcal{N}} [\, \lambda_n \,]^*|_h \cdot [\, p^g_n \,]^*|_h \,, \tag{3}$$

and the total hourly demand-side payments are

$$w^{\mathcal{B}}|_h \ = \sum_{n \in \mathcal{N}} [\, \lambda_n \,]^*|_h \cdot [\, p^d_n \,]^*|_h \,. \tag{4}$$

The hourly congestion rents are given by the difference between $w^{\mathcal{B}}|_h$ and $w^{\mathcal{S}}|_h$:

$$\kappa|_h \ = \sum_{n \in \mathcal{N}} [\, \lambda_n \,]^*|_h \cdot \Big([\, p^d_n \,]^*|_h - [\, p^g_n \,]^*|_h \Big) \,. \tag{5}$$

In the event that $\mathcal{M}(\mathcal{S}, \mathcal{B})\,|_h$ has no feasible solution because the fixed demand requirements cannot be satisfied due to shortfall in total generation capacity, some fraction of the fixed load at a subset of the nodes cannot be supplied, leading to a *loss of load* event. The *IGO* determines the unserved load $u_n|_h$ at each node n in the subset. Then, the total unserved demand due to loss of load in hour h is given by

$$\mathcal{U}|_h \ = \sum_{n \in \mathcal{N}} u_n|_h \,. \tag{6}$$

Clearly, whenever $\mathcal{M}(\mathcal{S}, \mathcal{B})\,|_h$ is feasible, $\mathcal{U}|_h = 0$. When $\mathcal{U}|_h > 0$, the *LMP*(s) at the node(s) with $u_n|_h > 0$ are set to the price cap λ^{max} and, then, the payments and congestion rents are evaluated. The metrics in (2)-(6) provide the measures of the market performance for an arbitrary hour h without *DRR* load curtailments or load recovery.

We need to make certain modifications to the market clearing problem in (1) to incorporate curtailment and recovery effects. We incorporate the impacts of *DRR*s as market players in each hour $h^c \in \mathcal{H}^c$ by extending the *DAM* representation and solving the *IGO*'s modified market clearing problem for the curtailment hours. By definition, a *DRR* is a buyer $b \in \mathcal{B}$ whose load curtailment cannot exceed his load in any hour $h^c \in \mathcal{H}^c$. We partition $\mathcal{B}$ into two non-overlapping subsets – the collection of buyers with demand response capability $\widehat{\mathcal{B}}$, and its complement $\bar{\mathcal{B}}$, the collection of *pure* buyers without demand response capability. Each *DRR* $\hat{b} \in \widehat{\mathcal{B}}$ is both a buyer purchasing electricity and a seller selling load curtailment. We represent these actions of *DRR* $\hat{b} \in \widehat{\mathcal{B}}$ in terms of its demand bid and its curtailment offer. The curtailment offer of *DRR* $\hat{b}$ consists of the maximum load it can curtail and the price at which the curtailment is provided. Whenever the hour h^c curtailment offer of a *DRR* is accepted, he becomes a *net* buyer and purchases only the net *MWh* for the remaining load after the load curtailment for that hour. Otherwise, he acts as pure buyer and purchases the *MWh* cleared in the market for its load without any curtailment.

The hour h^c market clearing determines the *DRR* load curtailment $\hat{p}^c_n$ at each node $n \in \mathcal{N}$ and the the aggregated costs incurred $\gamma^b_n(\cdot)$ by the *IGO* for the accepted *DRR* offers at node n. Note that the term $(p^d_n - \hat{p}^c_n)$ represents the net load cleared at that node. So, we use the vector $\underline{\hat{\boldsymbol{p}}}^c \triangleq [\, \hat{p}^c_1, \hat{p}^c_2, \ldots, \hat{p}^c_N \,]^T$

[1] We use the terminology auction surplus instead of social welfare because the offer (bid) data for the sellers (buyers) need not necessarily reflect the true costs (benefits) of the players.

and the term $\hat{p}_0^c$ in the equations (1b) and (1c) that represent the nodal power balance constraints and the cost term $\gamma_n^{\hat{b}}(\cdot)$ in (1a) to state the market clearing problem for the hour $h^c \in \mathcal{H}^c$, again with the hour h^c notation suppressed. We denote the hour h^c *OPF* by $\mathcal{M}(\mathcal{S}, \widehat{\mathcal{B}} \cup \bar{\mathcal{B}})\,|_{h^c}$, where we use the fact $\mathcal{B} = \widehat{\mathcal{B}} \cup \bar{\mathcal{B}}$ to explicitly represent the *DRR* players. We use the solution of $\mathcal{M}(\mathcal{S}, \widehat{\mathcal{B}} \cup \bar{\mathcal{B}})\,|_{h^c}$ to find the market clearing quantities for the hour h^c. Although each *DRR* provides a load curtailment service, it is compensated on a *\$/MWh* basis as if it provided the energy saved by its curtailment. The *IGO* recovers the compensation payments for the *DRR*s by collecting an additional curtailment service charge υ *\$/MWh* from all the buyers whose demand bids get cleared in the hour h^c market. Therefore, a buyer at the node n pays $\left([\lambda_n]^*|_{h^c} + \upsilon|_{h^c}\right)$ *\$/MWh* for his electricity purchases in the hour h^c. The value of $\upsilon|_{h^c}$ depends on the specific compensation scheme used. Assuming that the *DRR*s are compensated at the corresponding *LMP*s, we compute the total compensation $w^{\widehat{\mathcal{B}}}|_{h^c}$ paid to the *DRR*s whose bids are accepted in the hour h^c as

$$w^{\widehat{\mathcal{B}}}|_{h^c} = \sum_{n \in \mathcal{N}} [\lambda]_n^*|_{h^c} \cdot [\hat{p}_n^c]^*|_{h^c}, \qquad (7)$$

so that the "uplift" for the *DRR* curtailments incurred by each buyer is

$$\upsilon|_{h^c} = \frac{w^{\widehat{\mathcal{B}}}|_{h^c}}{\ell^{\mathcal{S}}|_{h^c}}. \qquad (8)$$

We use the nodal market clearing quantities and the uplift charge to evaluate the metrics (2)-(6) for each hour $h^c \in \mathcal{H}^c$.

Since the load curtailment by the *DRR*s whose offers are accepted in the hour $h^c \in \mathcal{H}^c$ may induce a deferred load in some subsequent hours in which the load recovery occurs [9], [10], the simulation needs to appropriately represent the *load recovery effects*. We use curtailment recovery factor (*CRF*) $\chi_{h^c,h^r}^{\hat{b}}$ to specify the fraction of *DRR* $\hat{b}$'s load curtailment in hour $h^c \in \mathcal{H}^c$ that is recovered in the hour $h^r \in \mathcal{H}^r$. The *CRF* is used to compute the recovery load p_n^r at each affected node $n \in \mathcal{N}$ [10]. Clearly, the term $(p_n^d + \hat{p}_n^r)$ represents the total load at the node n with the load recovery effects taken into account for hour h^r. Then, we can use the vector $\underline{\hat{\boldsymbol{p}}}^r \triangleq [\hat{p}_1^r, \hat{p}_2^r, \ldots, \hat{p}_N^r]^T$ and p_0^r to formulate the market clearing problem $\mathcal{M}(\mathcal{S}, \widehat{\mathcal{B}} \cup \bar{\mathcal{B}})\,|_{h^r}$ for the hour h^r. We use the solutions of $\mathcal{M}(\mathcal{S}, \widehat{\mathcal{B}} \cup \bar{\mathcal{B}})\,|_{h^r}$ to evaluate the market performance for each hour $h^r \in \mathcal{H}^r$ by using the suitably modified expressions of (2)-(6).

The hourly market clearing problem and the metrics defined using its solution serve as the basic building block in the quantification of the impacts of *DRR*s. We aggregate the variable effects for all the H hours in set $\mathcal{H}$ to quantify the variable effects of the entire simulation period. However, whenever a simulation involves future time periods, we need to explicitly consider the various sources of uncertainty which impact the operations of the markets and the system. We apply well-known probabilistic simulation notions to capture the uncertainty impacts on the system variable effects [17], [19].

We take into account the uncertainty due to the variability of the loads, the availability of the *SR*s and the clearing of the transmission-constrained markets. Under the set of adopted assumptions, we view the load over the simulation period as a random variable (*r.v.*) $\underset{\sim}{L}$ and use the forecasted hourly load data $\{\ell|_h : \forall\, h \in \mathcal{H}\}$ to estimate its cumulative distribution function (*c.d.f.*). Similarly, we use the discrete *r.v.* $\underset{\sim}{A}^i$ to represent the multi-state capacities for loading the *SR* $i \in \mathcal{I}$, where $\mathcal{I}$ represents the set of *SR*s in the system. We denote by $\alpha^i|_h$ the realization of $\underset{\sim}{A}^i$ for the hour h.

Now, the offers and the bids of the players for a particular hour h in the simulation period depend on the realizations $\ell|_h$ and $\alpha^i|_h$'s of the load and the available generation capacities, respectively. The uncertain load and available capacities result in uncertain market clearing outcomes, which we represent as *r.v.*'s. We denote the cleared load that is met by the supply resources by $\underset{\sim}{L}^{\mathcal{S}}$, the generation output of *SR* i by $\underset{\sim}{P}^i$, the node n *LMP* by $\underset{\sim}{\Lambda}_n$, the supply-(demand-)side payments by $\underset{\sim}{W}^{\mathcal{S}}$ ($\underset{\sim}{W}^{\mathcal{B}}$), the congestion rents by $\underset{\sim}{\mathcal{K}}$ and the unserved demand by $\underset{\sim}{\mathcal{U}}$. We use the outcomes of the hourly markets operated in the simulation period to approximate the *c.d.f.*'s of each of these *r.v.*'s.

We quantify the variable effects of the system by evaluating the expected values of the market outcome *r.v.*'s. The expected supply-side payments for the simulation period are denoted by $\mathscr{W}^{\mathcal{S}}$ with

$$\mathscr{W}^{\mathcal{S}} = H \cdot \mathbb{E}\left\{\underset{\sim}{W}^{\mathcal{S}}\right\}. \qquad (9)$$

We use analogous expressions to evaluate the expected demand-side payments $\mathscr{W}^{\mathcal{B}}$ and the expected congestion rents $\mathscr{K}$. We compute the expected energy supplied by *SR* $i \in \mathcal{I}$ for the simulation period using

$$\mathcal{E}^i = H \cdot \mathbb{E}\left\{\underset{\sim}{P}^i\right\}. \qquad (10)$$

We compute the contribution of the *SR* i to the expected emissions of the system over the simulation period using $\mathcal{E}^i$. We incorporate the impacts of *DRR* curtailments, market clearing and transmission constraints in the computation of the reliability metrics by using the unserved demand *r.v.* $\underset{\sim}{\mathcal{U}}$ to compute the loss of load probability $LOLP$,

$$LOLP = \mathbb{P}\left\{\underset{\sim}{\mathcal{U}} > 0\right\}, \qquad (11)$$

and expected unserved energy $\mathscr{U}$,

$$\mathscr{U} = H \cdot \mathbb{E}\left\{\underset{\sim}{\mathcal{U}} \,|\, \underset{\sim}{\mathcal{U}} > 0\right\} \cdot LOLP. \qquad (12)$$

We use these economic measures and the reliability metrics to evaluate the complete set of variable effects of interest.

We construct the proposed simulation approach making use of the hourly snapshot-based market clearing and the probabilistic models described in this section. We describe the approach in the next section.

III. Proposed Approach

In this section, we describe the proposed approach to emulate, over longer-term periods, the operations of the power system and electricity markets with *DRR*s and to quantify the system variable effects. An important requirement is the explicit consideration of the time-varying nature of *DRR* deployments and the representation, with appropriate level of detail, of the loads and resources, transmission grid, the market clearing operations, the market structure and various sources of uncertainty. We discuss the approach for a single simulation period for which the assumptions in section II are satisfied.

Conceptually, the market clearing for each hour h in the simulation period is performed for the particular realizations of $\underset{\sim}{L}$ and $\underset{\sim}{A}^{i}$, the demand and supply *r.v.*'s. The realization ℓ of $\underset{\sim}{L}$ manifests itself in terms of the sum of the fixed price load and price-sensitive bids submitted by the buyers, The realization α^{i} of $\underset{\sim}{A}^{i}$ represents the maximum capacity each unit $i \in \mathcal{I}$ offers in the market. In the absence of strategic behavior, the capacity α^{i} is offered to the market. In the event of a forced outage, $\alpha^{i} = 0$ and so unit i cannot contribute towards meeting the load in hour h. Indeed, the load sample ℓ and the sampled available capacities α^{i} are used to construct demand and supply curves, respectively, for the hour h market. Since the solution of $\mathcal{M}(\mathcal{S}, \widehat{\mathcal{B}} \cup \bar{\mathcal{B}})|_{h}$ is used to compute the realization of each market outcome *r.v.* – $\underset{\sim}{L}^{\mathcal{S}}$, $\underset{\sim}{P}^{i}$, $\underset{\sim}{\Lambda}_{n}$, $\underset{\sim}{W}^{\mathcal{S}}$, $\underset{\sim}{W}^{\mathcal{B}}$, $\underset{\sim}{K}$ and $\underset{\sim}{\mathcal{U}}$ – corresponding to the realized values of $\underset{\sim}{L}$ and $\underset{\sim}{A}^{i}$, we may view the *OPF* $\mathcal{M}(\mathcal{S}, \widehat{\mathcal{B}} \cup \bar{\mathcal{B}})|_{h}$ as mapping the realizations ℓ and α^{i} – the *input* – into the realizations $\ell^{\mathcal{S}}$, p^{i}, λ_{n}, $w^{\mathcal{S}}$, $w^{\mathcal{B}}$, κ and $\mathcal{U}$ of the corresponding market outcome *r.v.*'s – the *output* – for each hour $h \in \mathcal{H}$. The resulting collection of the market outcome realizations constitutes the sample space that we use to approximate the *c.d.f.*'s of the market outcome *r.v.*'s. In Fig. 1, we illustrate the basic steps in the approximation of each *c.d.f.* of interest used in the evaluation of the metrics in (9)-(12).

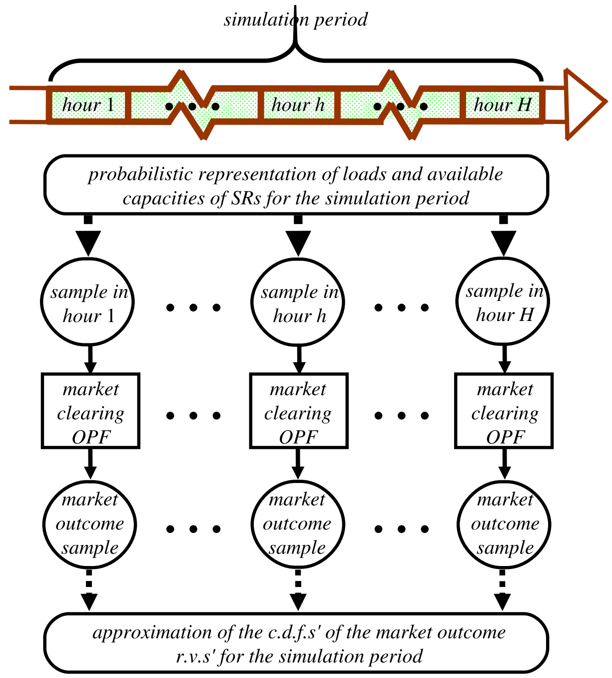

Fig. 1. Conceptual illustration of the scheme to construct the *c.d.f.*'s of the market outcome *r.v.*'s

Clearly, the solution of $\mathcal{M}(\mathcal{S}, \widehat{\mathcal{B}} \cup \bar{\mathcal{B}})|_{h}$ for the hour $h \in \mathcal{H}$ depends on whether hour $h \in \mathcal{H}^{c}$ or $h \in \mathcal{H}^{r}$ or $h \notin \mathcal{H}^{c} \cup \mathcal{H}^{r}$ and on the load curtailment capacity offered/associated load recovery effects. The *DRR* time-dependent nature and that of the market clearing require their representation in the simulation. This requirement precludes the direct application of the conventional probabilistic simulation framework [17], [19] in which time is abstracted out. As the load $\underset{\sim}{L}$ lacks temporal information, a modification of the probabilistic simulation is necessary to incorporate the impacts of *DRR* deployment. The modification makes use of the known hourly loads and the *DRR* usage schedule, be it for a typical weekday and a typical weekend day. We make use of the uniform load characteristics exhibited over the entire simulation period, i.e., in every hour of that period, to incorporate the effects of the time-varying *DRR*s. In fact, the probability distribution of the load *r.v.* $\underset{\sim}{L}$ holds for every hour in the period so that the approximate *c.d.f.* of $\underset{\sim}{L}$ is constructed from the collection of sampled load values for each hour $h \in \mathcal{H}$. Therefore, we can partition the collection of the hourly load samples $\{\ell|_{h} : h \in \mathcal{H}\}$ into 24 weekday hour subsets and 24 weekend day hour subsets, and use these subsets to approximate the conditional *c.d.f.* of $\underset{\sim}{L}$ conditioned on each such hour. Indeed, we can use load samples from the partition subsets to construct corresponding subsets of market outcome realizations obtained via the *OPF* $\mathcal{M}(\mathcal{S}, \widehat{\mathcal{B}} \cup \bar{\mathcal{B}})|_{h}$ mapping and approximate the conditional *c.d.f.*'s of the market outcome *r.v.*'s conditioned on each such hour. The *c.d.f.*'s of the market outcome *r.v.*'s are approximated as the probability weighted average of the conditional *c.d.f.*'s for the 24 weekday and 24 weekend hours. The details on the hourly conditioning and *c.d.f.* evaluation are presented in [6, pp. 53-67]. We construct the proposed approach through the systematic application of the hourly conditioning scheme.

We implement the proposed approach to quantify the variable effects of a power system with *DRR*s. The approach effectively captures the interactions between the *DRR* deployments, generation dispatch, transmission usage and congestion, market structure and market clearing outcomes under the specific policies in effect. The explicit representation of the various sources of uncertainty provides a realistic emulation of the hour-by-hour operation of the actual system over the simulation period. We do need to manage effectively the computing burden associated with the simulation of a large-scale system over a longer-term period. We describe in the next section the steps that need to be taken to ensure computational tractability in implementing the approach.

IV. Implementational Aspects

In this section, we discuss the implementational aspects of the proposed approach by focussing on the steps taken to ensure its computational tractability and make practical its application to the simulation of large-scale systems over longer-term periods. For a study spanning multiple years, we first partition the *study period* into T non-overlapping *simulation periods* to capture seasonal effects, changes in the resource mix and the transmission grid, maintenance schedules as well as the introduction of new policies. Any change entails the specification of a new simulation period and the introduction of the assumption that the change persists over that entire simulation period. As such, the simulation periods may be of unequal duration. We denote the index set of the non-overlapping simulation periods by $\mathscr{T} \triangleq \{1, \ldots, T\}$. We apply the proposed approach to each of the T simulation periods and aggregate the variable effects for these simulation periods (taking into account the time value of money where appropriate) to compute the variable effects for the study period.

To make the computing tasks tractable, we choose judiciously the simulation periods for a study and use numerically efficient computation of the hourly snapshots in each simulation period. Typically, we specify the simulation periods to be 168-hour weeks. Then, the set $\mathscr{T}$ consists of $52 \cdot y$ indices, where y is the number of years in the study period. Now, we can take advantage of the fact that several weeks in a year have similar load patterns because of the seasonal nature of electricity demand. So, we can use representative weeks to reduce the number of simulations below $52 \cdot y$. However, since the set of *SR*s on scheduled maintenance may differ across the weeks with similar load patterns, the number of representative weeks increases. The index set of the subset of the selected representative weeks is $\mathscr{T}' \subset \mathscr{T}$. We associate with each representative week $t' \in \mathscr{T}'$ a corresponding number, $\psi_{t'}$, of weeks it represents and apply the proposed approach to simulate each representative week $t' \in \mathscr{T}'$. The resulting assessments for that week are weighted by $\psi_{t'}$ to compute its contribution to the study period variable effects. In this way, we simulate representative weeks in the study period to effectively reduce the computations required.

We can further implement numerically efficient schemes for the simulation of each representative week. The approximation of the market outcome *r.v.*'s *c.d.f.*'s for a representative week entails extensive computations to take into account the many possible input sample realizations corresponding to the realized values of the demand and supply *r.v.*'s. In particular, each mapping of input sample of ℓ and α^i into the corresponding output sample of realization of the market outcome *r.v.*'s involves the solution the *OPF* problem with a large number of decision variables. Clearly, large-scale systems with several hundred generators and transmission lines impose major demands on computing resources. Consequently, we need an effective sampling technique to produce input sample realizations which are representative of all the possible realizations of the demand and supply *r.v.*'s.

Latin hypercube sampling or *LHS* [20] is a variance reduction technique that uses a stratified sampling approach to produce multiple samples realizations for a set of *r.v.*'s with known distributions. To obtain M sample realizations of a *r.v.*, we partition the domain of the *c.d.f.* of the *r.v.* into equal probability M intervals. Then, M realizations of the *r.v.* are chosen, one from each such interval. When sampling across multi-variate distributions of a set of demand and supply *r.v.*'s, we perform *LHS* on each component *r.v.* and obtain M sample realizations of each *r.v.* We then construct M input samples by pairing the sampled values of each component *r.v.* The pairing scheme depends on the correlations and dependence between the component *r.v.*'s [21]. The M sample realizations of the demand and the supply *r.v.*'s result in a computationally efficient approximation of the *c.d.f.*'s of the market outcome *r.v.*'s and their expected values [22]. Unlike random sampling, the stratified sampling approach of the *LHS* ensures that the entire distribution of the demand and supply *r.v.*'s – including the extreme regions of the *c.d.f.*'s – is sampled for the reliability assessments, providing useful means for evaluating the reliability metrics $LOLP$ and $\mathscr{U}$ [23]. To choose an appropriate sample size M, we use a frequently-employed rule of thumb and require that the sample size be larger than the number of *r.v.*'s being sampled by a factor η, where $\eta \in [1.5, 20]$. Our extensive testing has borne out that this rule of thumb is useful for the large-scale systems we tested.

The judicious selection of representative simulation periods and the use of *LHS* technique to build statistically representative sample realizations of the demand and supply *r.v.*'s for the approximation of the *c.d.f.*'s of the market outcome *r.v.*'s bring about computational tractability in the implementation of the proposed approach. This implementation strategy for the proposed approach is particularly effective in the study of large-scale systems over longer-term periods. We illustrate, in the next section, the application of our approach with the implementational scheme to answer a wide variety of *what-if* questions for planning and policy analysis.

V. Application Studies

We illustrate the application of the proposed simulation approach to a set of studies on a large-scale test system. The goal of these studies is to investigate the ramifications of the integration of *DRR*s into the power system. We investigate the impacts of varying levels of *DRR* penetration and load recovery effects and analyze the economic, environmental and reliability benefits associated with the effective utilization of *DRR*s. The results discussed here are representative of those in our extensive tests of the proposed approach. These results demonstrate the capabilities of the proposed approach to study various power system planning and policy analysis issues.

The test system we use for the simulations consists of 241 buses and 555 transmission lines and is representative of large-scale *ISO* networks. We explicitly consider the constraints imposed by the real power transfer capabilities of the transmission grid. There are loads connected at 130 buses in the network. We use the historical load shapes of the Midwest *ISO* system for the year 2006 [24]. The aggregate average hourly load for the system is 70 *GW*, with the annual peak load of 117 *GW* in the summer. There are generators connected at 152 buses in the network. The supply-side resource mix capacity composition is given in Table I. The supply system consists of 766 generators. Each generation unit has a pre-specified maintenance schedule. We use the emissions factors in [25] to estimate the expected CO_2 emissions from the supply-side generation.

TABLE I
THE CAPACITY COMPOSITION OF THE SUPPLY-SIDE RESOURCE MIX IN *GW*

coal	CCGT	peakers	others	total
70	21	24	20	135

We designate some of the loads in the system as *DRR*s. We use the total *DRR* capacity – expressed as a fraction of the annual system peak load – as the penetration level parameter and study the impacts of varying *DRR* penetration levels. The impacts of the load recovery consequences for the *DRR* curtailments are studied by varying the associated *CRF*s $\chi^{\hat{b}}_{h^c,h^r}$'s. In the simulations reported here, we consider each buyer as submitting fixed demand bids in the hourly *DAM*s. We limit the hours *DRR*s can offer load curtailments in the *DAM*s from the hour ending at 9:00 to the hour ending at 18:00 for each weekday. The load recovery hours are from the hour ending at 23:00 to the hour ending at 6:00.

We limit our analysis to a single year to get insights into the nature of results obtained. The seasonality effects, the load patterns and the maintenance scheduling requirements allow us to reduce the 52 weeks in the year to 15 representative weeks. Each representative week weight is at least $1/52$. In the *LHS* deployment, we select sample sizes between 500 and 1000. We use the test system simulation without the *DRR*s, which we denote as $\mathbb{D}_0$, to provide the variable effects for the reference case of our studies. We assess the impacts of the *DRR*s with respect to the variable effects in $\mathbb{D}_0$. These are summarized in Table II.

TABLE II
VARIABLE EFFECTS OF CASE $\mathbb{D}_0$ FOR THE SIMULATED YEAR

min, avg and max values of the cleared load (*GW*)		average values of the economic metrics	
base load	50.806	electricity payments	$ 4.453 M
average load	69.910	congestion rents	$ 67,752
peak load	117.658	CO_2 emissions	11,823 tons

We discuss first the implementation of *DRR*s into the test system with a total capacity of 5.6 *GW*, which is approximately 5 % of the peak load. We examine two specific cases: $\mathbb{D}_{05,00}$ without recovery of the *DRR* curtailments and $\mathbb{D}_{05,70}$ with 70 % recovery of the curtailments offered and accepted in the *DAM*s. We summarize the load-related metrics for each of these cases in Table III from which we can evaluate the effect of *DRR*s on reducing the loads in the peak load hours of the study period. The reduction in the load is observed

TABLE III
MINIMUM, AVERAGE AND MAXIMUM VALUES FOR THE HOURLY CLEARED LOADS IN *GW*

case	base load	average load	peak load
$\mathbb{D}_{05,00}$	50.806	69.830	112.720
$\mathbb{D}_{05,70}$	52.242	69.575	112.720

in approximately 25 % of the hours in the year. The load reduction results in a visible downward shift in the load duration curve (*LDC*), as shown in Fig. 2. Note the *LDC*

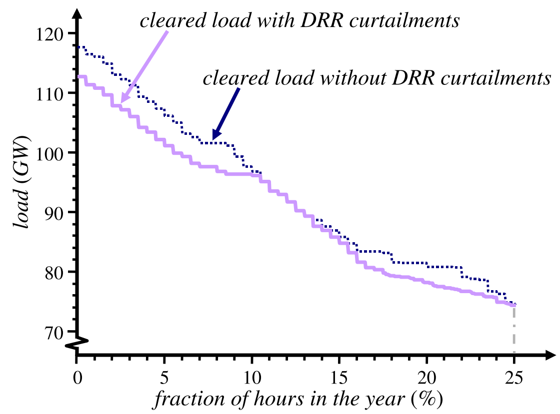

Fig. 2. The impacts of *DRR* curtailments on the cleared loads for the peak hours of the year as seen from the high load portion of the annual *LDC*

shown here is constructed using the hourly cleared loads. The reduction in the annual peak load from 117.658 to 112.720 *GW* increases the capacity margin of the system by 5 %; from 14.74 to 19.77 %. When the load recovery effects are considered in case $\mathbb{D}_{05,70}$, the increases in the cleared loads during the off-peak hours lead to an upward shift in the *LDC*, including a larger base load value, as shown in Fig. 3. The

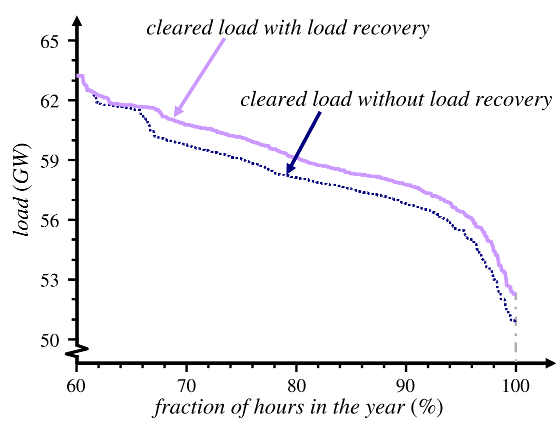

Fig. 3. The impacts of *DRR* curtailment recovery during the off-peak hours of the year as seen from the low load portion of the annual *LDC*

DRR-provided peak shaving results in a number of important economic and environmental benefits as measured by the electricity payments, congestion rents and CO_2 emissions. We tabulate the average values of these metrics for the $\mathbb{D}_{05,00}$ and $\mathbb{D}_{05,70}$ cases in Table IV. The *DRR* reduced system loads during the peak hours decrease the *LMP*s in those hours, which in turn, reduce the annual electricity payments of all the buyers by nearly as much as 11%. We note that the congestion rents in these two *DRR* cases are significantly lower than the reference case – by as much as 35% – indicating that the *DRR* deployments can drastically impact network flows and provide transmission congestion relief. Moreover, the decrease in the energy consumption implies that the generation for the system is also reduced, and hence we have a decrease in the CO_2 emissions.

TABLE IV
AVERAGE VALUES FOR THE HOURLY METRICS

case	electricity payments (M$)	congestion rents ($)	CO_2 emissions (tons)
$\mathbb{D}_{05,00}$	4.069	44, 350	11, 574
$\mathbb{D}_{05,70}$	4.150	45, 515	11, 738

To assess the impacts of *DRR* penetration and load recovery effects, we simulate cases with varying capacity of *DRR*s and different values of the *CRF*s $\chi^{\hat{b}}_{h^c,h^r}$'s. We illustrate in Fig. 4 that as *DRR* penetration deepens, the capacity margin increases and the aggregate annual congestion rents decrease. Since the *DRR* provided peak load reduction is not impacted by load recovery, the capacity margin depends on the level of *DRR* penetration. The total congestion rents collected by the *IGO* during the year are impacted by both the amount of load curtailed and the amount of load recovered by the *DRR*s. As the load recovery effects become more pronounced, the reduction in the congestion rents with deeper *DRR* penetration decreases markedly. Similar plots are available to illustrate the nature of the total annual electricity payments. While the energy savings decrease as more load is recovered, the total electricity payments in *DRR* cases with different penetration levels and load recovery effects remain lower than those in the reference case $\mathbb{D}_0$. Shifting the load from peak to off-peak hours due to *DRR* deployment results in the utilization of more economic generation resources. Therefore, not withstanding the load recovery effects, a deeper *DRR* penetration results in economic benefits in terms of reduced electricity payments and congestion rents, representing the more efficient utilization of the generation and transmission resources.

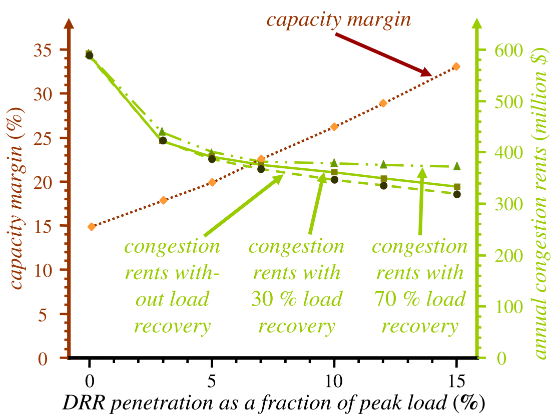

Fig. 4. The impacts of deeper *DRR* penetration and load recovery effects on the system capacity margin and congestion rents

We also investigate the ability of *DRR*s to defer the need for additional generation capacity. We compare the $\mathbb{D}_0$ and $\mathbb{D}_{05,00}$ cases under a 3 % load growth scenario and no additions to/retirements from the supply-side resource mix. We compute the hourly cleared loads in these cases and compare them to the forecasted loads. We note a capacity shortage in 2 % of the hours of the year for the reference case $\mathbb{D}_0$ and resulting loss of load at some nodes. However, no shortage of capacity arises in the $\mathbb{D}_{05,00}$ case due to the reduced loads during the peak hours. The illustration in Fig. 5

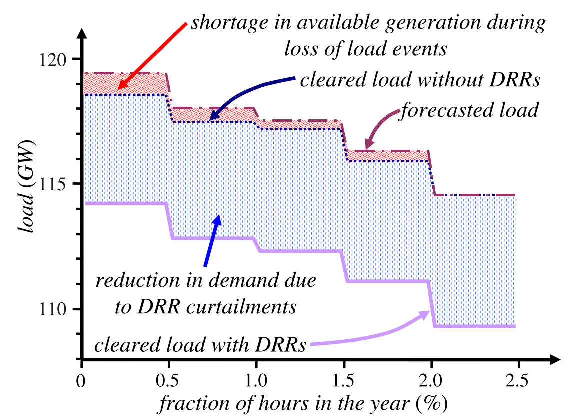

Fig. 5. Reduction in loss of load events due to *DRR* deployment

clearly indicates the capacity shortage in the peak load hours in $\mathbb{D}_0$. Such shortage effects may be overcome by adding approximately 1 *GW* of peaking capacity. Clearly, the effective use of *DRR*s is able to defer the need for such additional capacity. Therefore, *DRR* curtailments can impact the need for additional generation capacity.

We also investigate the impacts of *DRR* deployments on the need for transmission reinforcement. We compute the aggregate annual congestion rents for the cases without *DRR*s and with 5 % *DRR* capacity for four different configurations of the transmission grid: the existing grid, the existing grid with line τ_a upgraded, the existing grid with lines τ_a and τ_b upgraded, and, the existing grid with lines τ_a, τ_b and τ_c upgraded. We plot the congestion rents in Fig. 6 for four different grid configurations for the two cases. For simplicity, we use *CRF*s $\chi^{\hat{b}}_{h^c,h^r} = 0$ in the 5 % *DRR* case but we obtain similar plots for other values of $\chi^{\hat{b}}_{h^c,h^r}$. We note from Fig. 6 that as more transmission lines are upgraded, the transfer capability of the system improves and we observe lower congestion rents for both cases – with and without

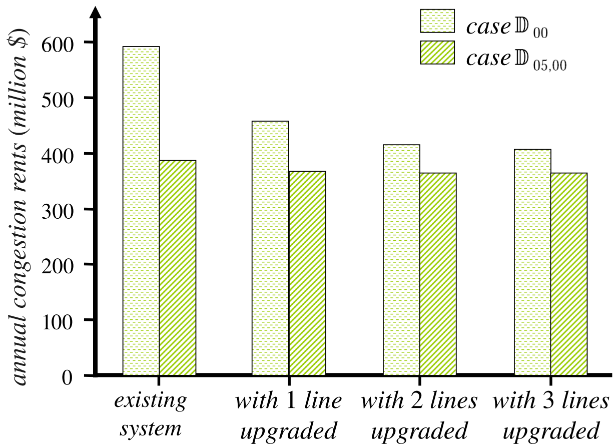

Fig. 6. Congestion rents for the system with transmission line upgrades in the $\mathbb{D}_{0}$ and $\mathbb{D}_{05,00}$

*DRR*s. A significant finding of this exercise is that the lowest congestion rents are $406 million for the system with 3 line upgrades for the reference case $\mathbb{D}_{0}$, which are higher than the congestion rents of $387 million on the existing transmission system for the *DRR* case $\mathbb{D}_{05,00}$. We observe similar results when load recovery effects are considered. We conclude, consequently, that effective utilization of the *DRR*s can lead to more reduction in the congestion rents than undertaking the capital intensive projects such as transmission line upgrades. Indeed, the integration of *DRR*s into the power system may defer the need for additional transmission and not only for new supply-side resources.

In each of the many cases studied, we have quantified the beneficial impacts of *DRR*s in reducing the system electricity payments, the transmission congestion and the loss of load probability. These benefits vary with the load recovery effects and the penetration of *DRR*s. Such quantification, as given in the representative results discussed, demonstrates the effectiveness of the proposed approach for use in a broad range of applications.

VI. Concluding Remarks

In this paper, we propose a simulation approach for evaluating the variable effects of power systems with integrated *DRR*s. The ability to quantify the impacts of *DRR*s on the economics of electricity supply, environmental effects of electricity production and reliability of the system makes the approach very useful in regulatory filing studies, long-term planning and policy analysis. We demonstrate the capability of the proposed approach to answer a broad range of *what-if* questions for a realistic-sized power system. We present results from extensive simulation studies which quantify impacts of *DRR*s on the system variable effects for different *DRR* penetration levels and varying load recovery characteristics. Our investigations provide practical insights into the significant role played by the *DRR*s in the efficient utilization of generation and transmission resources and in increased competition in the electricity markets to bring about lower prices to consumers.

As the penetration of renewable resources – such as wind and solar – deepens, the simulation approach proposed here needs to be extended to include their impacts on the system and market operations. The modeling must carefully represent the lack of control capability and the intermittency effects associated with the renewable generation along with the uncertainty associated with prediction of the wind/solar output patterns. In addition, energy storage units – be they utility-scale storage devices or large aggregations of plug-in hybrid electric vehicles – whose flexibility can be effectively harnessed in the management of the intermittent renewable resources need to be explicitly represented. The studies extending the proposed approach to incorporate renewables, storage and other time-dependent resources will be reported in future publications.

Acknowledgment

The research is supported in part by the Grainger Endowments to the University of Illinois and the Department of Energy under Award Number DE-OE0000097. The authors thankfully acknowledge the support and encouragement of Dr. Ralph Masiello, Dr. Alan Roark, Dr. Mimi Goldberg and others at KEMA, Inc in conducting this research.

References

[1] R. Masiello, “Demand response: The other side of the curve [guest editorial],” *Power and Energy Magazine, IEEE*, vol. 8, no. 3, pp. 18 –18, may-june 2010.

[2] L. Ruff, “Economic principles of demand response in electricity,” Tech. Rep., October 2002, prepared for Edison Electric Institute, Washington, D.C.

[3] U. S. Department of Energy, “Benefits of demand response in electricity markets and recommendations for achieving them,” February 2006. [Online]. Available: {http://www.oe.energy.gov/DocumentsandMedia/congress_1252d.pdf}

[4] FERC Staff, “Assessment of demand response and advanced metering,” Federal Energy Regulatory Commission, Tech. Rep., December 2008. [Online]. Available: http://www.ferc.gov/legal/staff-reports/12-08-demand-response.pdf

[5] A. Faruqui, R. Hledik, S. Newell, and H. Pfeifenberger, “The power of 5 percent,” *The Electricity Journal*, vol. 20, no. 8, pp. 68–77, October 2007.

[6] A. Kowli, “Assessment of variable effects of systems with demand response resources,” Master’s thesis, Department of Electrical and Computer Engineering, University of Illinois at Urbana-Champaign, 2009. [Online]. Available: http://energy.ece.uiuc.edu/gross/papers/Dissertations/Kowli.pdf

[7] K. Hamilton and N. Gulhar, “Taking demand response to the next level,” *Power and Energy Magazine, IEEE*, vol. 8, no. 3, pp. 60 –65, may-june 2010.

[8] “A national assessment of demand response potential,” Federal Energy Regulatory Commission, Tech. Rep., June 2009. [Online]. Available: http://www.ferc.gov/legal/staff-reports/06-09-demand-response.pdf

[9] G. Strbac, E. Farmer, and B. Cory, “Framework for the incorporation of demand-side in a competitive electricity market,” *IEE Proceedings - Generation, Transmission and Distribution*, vol. 143, no. 3, pp. 232–237, May 1996.

[10] A. Borghetti, G. Gross, and C. A. Nucci, “Auctions with explicit demand-side bidding in competitive electricity markets,” in *The Next Generation of Electric Power Unit Commitment Models*, B. F. Hobbs, M. H. Rothkopf, R. P. O’Neill, and H. po Chao, Eds. Norwell, MA: Kluwer Academic Publishers, 2001, vol. 36, pp. 53–74.

[11] C.-L. Su and D. Kirschen, “Quantifying the effect of demand response on electricity markets,” *IEEE Transactions on Power Systems*, vol. 24, no. 3, pp. 1199–1207, August 2009.

[12] R. Walawalkar, S. Blumsack, J. Apt, and S. Fernands, "Analyzing PJM's economic demand response program," in *2008 IEEE Power and Energy Society General Meeting - Conversion and Delivery of Electrical Energy in the 21st Century*, July 2008, pp. 1–9.

[13] E. Bompard, R. Napoli, and B. Wan, "The effect of the programs for demand response incentives in competitive electricity markets," *European Transactions on Electrical Power*, vol. 19, no. 1, pp. 127–139, January 2009.

[14] V. Stanojevic, V. Silva, D. Pudjianto, G. Strbac, P. Lang, and D. Macleman, "Application of storage and demand side management to optimise existing network capacity," in *Electricity Distribution, 2009 20th International Conference and Exhibition on*, June 2009, pp. 1 –4.

[15] R. Earle, E. P. Kahn, and E. Macan, "Measuring the capacity impacts of demand response," *The Electricity Journal*, vol. 22, no. 6, pp. 47 – 58, July 2009.

[16] S. Stoft, *Power System Economics: Designing Markets for Electricity*. New York, NY: Wiley-IEEE Press, 2002.

[17] A. J. Wood and B. F. Wollenberg, *Power Generation, Operation and Control*, 2nd ed. New York, NY: John Wiley and Sons, Inc., 1996.

[18] M. Liu and G. Gross, "Framework for the design and analysis of congestion revenue rights," *IEEE Transactions on Power Systems*, vol. 19, no. 1, pp. 243–251, Feb. 2004.

[19] R. Sullivan, *Power System Planning*. New York, NY: McGraw Hill International Book Company, 1977.

[20] M. McKay, R. Beckman, and W. Conover, "Comparison of three methods for selecting values of input variables in the analysis of output from a computer code," *Technometrics*, vol. 21, no. 1, pp. 239–245, 1979.

[21] M. Stein, "Large sample properties of simulations using latin hypercube sampling," *Technometrics*, vol. 29, no. 2, pp. 143–151, 1987.

[22] J. Linderoth, A. Shapiro, and S. Wright, "The empirical behavior of sampling methods for stochastic programming," *Annals of Operations Research*, vol. 142, pp. 219 – 245, 2006.

[23] P. Jirutitijaroen and C. Singh, "Comparison of simulation methods for power system reliability indexes and their distributions," *IEEE Transactions on Power Systems*, vol. 23, no. 2, pp. 486–493, May 2008.

[24] Midwest ISO staff, archived data in the Market Reports Section on the Midwest ISO website, July 2008. [Online]. Available: http://www.midwestiso.org/publish/Folder/7be606_10b7aacd66e_-7da30a48324a?rev=6

[25] S. Meyers, C. Marnay, K. Schumacher, and J. Sathaye, "Estimating carbon emissions avoided by electricity generation and efficiency projects: A standardized method," Lawrence Berkeley National Laboratory, Berkeley, CA, Tech. Rep. LBNL-46063, July 2000. [Online]. Available: http://eetd.lbl.gov/ea/ems/reports/46063.pdf